



Role of cathepsin B of *Naegleria fowleri* during primary amoebic meningoencephalitis

Itzel Berenice Rodríguez-Mera¹ · María Maricela Carrasco-Yépez² · Ismael Vásquez-Moctezuma³ · José Correa-Basurto⁴ · Gema Ramírez-Salinas⁴ · Diego Arturo Castillo-Ramírez¹ · Érika Rosales-Cruz⁵ · Saúl Rojas-Hernández¹

Received: 17 June 2022 / Accepted: 6 September 2022 / Published online: 20 September 2022
© The Author(s), under exclusive licence to Springer-Verlag GmbH Germany, part of Springer Nature 2022

Abstract

Naegleria fowleri causes primary amoebic meningoencephalitis in humans and experimental animals. It has been suggested that cysteine proteases of parasites play key roles in metabolism, nutrient uptake, host tissue invasion, and immune evasion. The aim of this work was to evaluate the presence, expression, and role of cathepsin B from *N. fowleri* in vitro and during PAM. Rabbit-specific polyclonal antibodies against cathepsin B were obtained from rabbit immunization with a synthetic peptide obtained by bioinformatic design. In addition, a probe was designed from mRNA for *N. fowleri* cathepsin B. Both protein and messenger were detected in fixed trophozoites, trophozoites interacted with polymorphonuclear and histological sections of infected mice. The main cathepsin B distribution was observed in cytoplasm or membrane mainly pseudopods and food-cups while messenger was in nucleus and cytoplasm. Surprisingly, both the messenger and enzyme were observed in extracellular medium. To determine cathepsin B release, we used trophozoites supernatant recovered from nasal passages or brain of infected mice. We observed the highest release in supernatant from recovered brain amoebae, and when we analyzed molecular weight of secreted proteins by immunoblot, we found 30 and 37 kDa bands which were highly immunogenic. Finally, role of cathepsin B during *N. fowleri* infection was determined; we preincubated trophozoites with E-64, pHMB or antibodies with which we obtained 60%, 100%, and 60% of survival, respectively, in infected mice. These results suggest that cathepsin B plays a role during pathogenesis caused by *N. fowleri* mainly in adhesion and contributes to nervous tissue damage.

Keywords cysteine proteases · cathepsin B · protease inhibitors · antibodies · *Naegleria fowleri*

Handling Editor: Una Ryan

✉ Saúl Rojas-Hernández
saulrohe@yahoo.com.mx

- ¹ Laboratorio de Inmunología Molecular, Instituto Politécnico Nacional, Escuela Superior de Medicina, Salvador Díaz Mirón Esq. Plan de San Luis S/N, Miguel Hidalgo, Casco de Santo Tomas, Ciudad de México, CDMX 11340, México
- ² Laboratorio de Microbiología Ambiental, Estado de México, Universidad Nacional Autónoma de México, Grupo CyMA, UIICSE, FES Iztacala, Tlalnepantla de Baz, México
- ³ Laboratorio de Bioquímica, Instituto Politécnico Nacional, Escuela Superior de Medicina, Ciudad de Mexico, México
- ⁴ Laboratorio de Modelado Molecular y Diseño de Fármacos, Instituto Politécnico Nacional, Escuela Superior de Medicina, Ciudad de Mexico, México
- ⁵ Instituto Politécnico Nacional, Escuela Nacional de Ciencias Biológicas, Ciudad de Mexico, México

Introduction

Infections caused by protozoa are among the main causes of death worldwide (Martínez-Castillo et al. 2016; Mishra et al. 2009). *Naegleria fowleri* Carter, 1970, *Acanthamoeba* spp Volkonsky, 1931, and *Balamuthia mandrillaris* Visvesvara, 1990, are the most common free-living amoebas (FLA) with medical implications, since they cause serious and fatal infections in the central nervous system (CNS) in many mammals, including humans (Martínez-Castillo et al. 2016; Visvesvara et al. 2007).

N. fowleri causes primary amoebic meningoencephalitis (PAM), a CNS disease which begins when trophozoites enter in the nasal cavity; once there, they adhere to olfactory epithelium, migrate through lamina propria next to olfactory nerves. It has been suggested that these nerves are used by amoeba to cross cribriform plate until they reach the olfactory bulbs

(OBs) and brain (Aurongzeb et al. 2021; Grace et al. 2015; Moseman 2020; Pugh and Levy 2016). Once the trophozoites are inside the brain, they begin to divide and phagocytize the nervous tissue, causing an acute inflammatory reaction, which leads to the death of the host in a period of 3–7 days (Jahangeer et al. 2020; Rojas-Hernández et al. 2004).

To understand the amoeba-host interaction, several *in vivo* studies have been carried out (Carrasco-Yepepe et al. 2019; Jaroli et al. 2002; Rojas-Hernández et al. 2004) to determine the mechanisms of immune evasion, adhesion, invasion, and damage to tissues caused by *N. fowleri* (Carrasco-Yepepe et al. 2013; Lee et al. 2014; Shibayama et al. 2013; Siddiqui et al. 2016; Vyas et al. 2015). Neuraminidases, elastases, lipases, hydrolases, phospholipases, and proteases have been related to the ability of *N. fowleri* to cause damage (Betanzos et al. 2019; Güémez and García 2021; Marciano-Cabral and Cabral 2007).

Specifically, proteases contribute to the pathogenicity of various microorganisms such as *Entamoeba histolytica* Schaudinn, 1903, *Giardia intestinalis* Kunstler, 1882, *Acanthamoeba* spp., *Trichomonas vaginalis* Donné, 1836, *Balamuthia mandrillaris*, and *Naegleria fowleri* (Lee et al. 2014; Piña-Vázquez et al. 2012; Serrano-Luna et al. 2013). This characteristic makes them an important virulence factor that can be considered as a target for antiparasitic drugs or vaccines.

In vitro studies have showed that cysteine proteases (CPs) of *N. fowleri* have approx. molecular weights of 30, 58, 128 and 170 kDa (Mat Amin 2004; Vyas et al. 2015). In addition, it was shown the presence of cathepsin B and cathepsin B-like proteases in supernatants of *N. fowleri* trophozoites (Kim et al. 2009). The same group cloned and purified these CPs with 38.4 and 34 kDa molecular weights, which showed proteolytic activity against immunoglobulins, fibronectin, collagen, albumin, and hemoglobin (Lee et al. 2014). Using a monoclonal antibody, Seong et al. (2017) reported that the main distribution of cathepsin B was in cytoplasm of *N. fowleri* trophozoites, particularly in pseudopods and food-cups. Taken together, the authors suggest that this protease may be involved with adhesion, host tissue invasion, and immune evasion.

The present study aims to elucidate the presence, expression, and distribution of cathepsin B in *N. fowleri* trophozoites alone, interacting with polymorphonuclear leucocytes (PMNs) and in infected mice as well as its role during pathogenesis in infected mice with trophozoites preincubated with specific inhibitors or antibodies against this enzyme.

Methodology

Naegleria fowleri culture

N. fowleri trophozoites (ATCC 30,808) were cultured under axenic conditions in Bactocasitone medium supplemented

with 10% heat-inactivated fetal bovine serum (Gibco) and 1% penicillin–streptomycin (Gibco) at 37 °C. Trophozoites were chilled and harvested during the logarithmic phase (48 h). After centrifuging at 1500 × g for 10 min, the supernatants were recovered and stored at -70 °C until use. The virulence of *N. fowleri* was reactivated by serial passage through mice as described previously by Rojas et al. (2004).

Animals

All procedures performed in this study, which involved Balb/c mice 6 to 8 weeks old as well as a New Zealand rabbit approximately 3 months old, were in accordance with the Mexican Federal regulations for animal experimentation and care (NOM 062-ZOO-1999, Ministry of Agriculture, Mexico City, Mexico) and approved by the ethical standard of Institutional Animal Care and Use Committee (Number of Approval ESM-CICUAL-ADEM-05/27–09-2019).

Design of a peptide from *N. fowleri* cathepsin B

First, we obtained *N. fowleri* cathepsin B sequence from the NCBI database (<http://www.ncbi.nlm.nih.gov/protein>) (GenBank: AHW50663) reported by Lee et al. (2014), to design a synthetic peptide for *N. fowleri* cathepsin B (SPCB-NF) by *in silico* investigation using comparative modeling and molecular dynamics simulation as reported by Loyola et al. (2013). Homology modeling was performed using the crystal structure of rat procathepsin B (PDB ID: 1MIR), recently reported by Aurongzeb et al. (2021). Peptide sequence chosen corresponds to amino acids 71–94 which was used to obtain polyclonal antibodies against SPCB-NF. After that, we performed a phylogenetic analysis of amino acid sequence of cathepsin B from various organisms. Phylogenetic tree was constructed by neighbor-joining method using MEGA 6 software (RRID:SCR_000667).

Obtention and purification of rabbit polyclonal antibodies against SPCB-NF

A rabbit was immunized three times with SPCB-NF: i) 200 µg of peptide plus complete Freund's adjuvant (Sigma Chemical Co.) was administered subcutaneously on day 1; ii) 200 µg of peptide plus incomplete Freund's adjuvant was administered by the same route on day 8; iii) 200 µg of peptide in 5 mL of saline solution was administered through the intramuscular route on day 15. Seven days after the last immunization, the rabbit was anesthetized with pentobarbital, and serum samples were obtained from blood extracted by cardiac puncture and stored at -70 °C until use. The specificity of antibodies against SPCB-NF was evaluated by immunodetection in mouse bone marrow PMNs by immunocytochemistry.

Rabbit anti-SPCB-NF purification

IgG from rabbit serum was purified by affinity chromatography using a protein A column (Thermo Scientific). Serum was diluted 1:1 in binding buffer (PBS: 10 mM Na₂HPO₄, 150 mM NaCl, pH 7.2) before applied to the column. Bound proteins were eluted with elution buffer (0.1 M glycine pH 2.5). The IgG fraction was dialyzed in PBS for 24 h at 4 °C and concentrated with an Amicon Ultra centrifugal filter unit tube (Sigma Aldrich); finally, protein concentration was determined by the Bradford method. Purified anti-SPCB-NF antibody was used in all experiments.

Mouse polymorphonuclear cells isolation

PMNs were obtained from the mice bone marrow of the upper and lower extremities. The isolation was performed by density gradient centrifugation method using Histopaque (Sigma-Aldrich) 1077 and 1119 solutions. The samples were centrifuged at 700 × g for 32 min at 20 °C. Cell viability and purity were evaluated by staining with trypan blue and Turk method (0.1% gentian violet in 0.1 M acetic acid), respectively, using a Neubauer chamber and light microscope (40x).

Immunocytochemistry

N. fowleri trophozoites (1 × 10⁶ cells/mL) or PMNs (1 × 10⁶ cells/mL) or trophozoites interacted with -PMNs (1:1) were incubated on glass coverslips in a 24-well plate for 1 h at 37 °C. After incubation, the samples were fixed with 4% paraformaldehyde (PFA, pH 7.3) for 30 min at 37 °C and blocked with 1% bovine serum albumin (BSA) (Research Organics) for 30 min at 37 °C. All samples were permeabilized with PBS-TT (10 mM Na₂HPO₄, 150 mM NaCl, 0.005% Tween-20 y 0.5% Tritón, pH 7.2) for 5 min at room temperature. For immunodetection, trophozoites were incubated overnight with anti-SPCB-NF antibody (1:100) for 24 h at 4 °C. After incubation, samples were washed three times with PBS and incubated with Donkey Anti-Rabbit IgG H&L (Alexa Fluor® 647) ab150075, RRID:AB_2752244 or Donkey Anti-Rabbit IgG H&L (Alexa Fluor® 488) ab150073, RRID:AB_2636877 (1:1000) for 24 h at 4 °C. For DNA detection, all samples were incubated with 4,6-diamidino-2-phenylindole (DAPI). Finally, coverslips were mounted with VECTASHIELD (Vector Laboratories, Inc.). Images were collected and analyzed with an Axioscop 2 mot plus confocal fluorescence microscope (Carl Zeiss).

Immunohistochemistry

Four mice were intranasally inoculated with 12,000 live *N. fowleri* trophozoites and euthanized 24 h after inoculation.

The skin of heads and the lower jaw was removed and then were fixed with PFA 4% for 24 h. Subsequently, the samples were washed with water and decalcified with 8% ethylenediaminetetraacetic acid (EDTA, pH 7.6) for 7 days. The samples were dehydrated with a train of alcohols and Xylol. Finally, the heads were included in paraffin blocks. After, we obtained 7-µm sections using a microtome (Leica RM2125). The sections were deparaffinated and hydrated in PBS. After that, samples were blocked with 5% BSA for 1 h and then incubated with anti-SPCB-NF antibody (1:100) for 24 h at 4 °C. Then, the samples were incubated with Donkey Anti-Rabbit IgG H&L (Alexa Fluor® 647) or Donkey Anti-Rabbit IgG H&L (Alexa Fluor® 488) for 24 h at 4 °C. All samples were incubated with DAPI. Finally, the samples were mounted with VECTASHIELD. Images were analyzed by confocal microscopy (Carl Zeiss).

Fluorescence in situ hybridization (FISH)

For detection of cathepsin B-mRNA, we selected one nucleotide sequence that contained 20 nucleotides including ten adenine–thymine and ten cytosine-guanine (reverse 5′-TATGGCATGCATGAGTCAGG-3′, cDNA position 577–596 [GenBank: KJ159026]) and the probe was labeled by Cy5. To determine the probe specificity, we performed phylogenetic analysis of mRNA sequences of cathepsin B from various organisms. The phylogenetic tree was constructed by neighbor-joining method using MEGA 6 software. To evaluate probe specificity in vitro, mouse bone marrow PMNs were incubated with designed probe against *N. fowleri* cathepsin B-mRNA.

To detect cathepsin B-mRNA in cells or tissues, FISH was performed as reported by Vásquez-Moctezuma et al. (2010). Briefly, samples were fixed and permeabilized as previously described. Afterward, prehybridization was done with 50% hybridol (Merck) and 50% formamide at 40 °C for 1 h. For mRNA detection, hybridization was done using 500 ng of probe at 80 °C for 5 min and 40 °C overnight. All samples were washed twice with citrates buffer (0.015 M NaCl and 0.0015 M sodium citrate) at room temperature for 1 h and two more with PBS.

Enzyme-linked immunosorbent assay

Release of cathepsin B from *N. fowleri* during PAM was determined by an indirect enzyme-linked immunosorbent assay (ELISA). Three groups of two mice were infected with 12,000 live trophozoites and euthanized 24, 48, and 72 h post-infection. Subsequently, nasal passages (NP) and brains (B) were recovered and incubated under axenic conditions in culture boxes for approximately 4 h. Once the trophozoites adhered to the plastic, the tissues were removed and the culture boxes were washed twice to remove tissue

remains or non-adhered cells. Afterward, the trophozoites were incubated for 24 h at 37 °C and harvested as previously described. The supernatants were recovered, and release of cathepsin B was evaluated. Briefly, 96-well plates were coated with 5 µg of supernatant from each time point (24, 48 or 72 h) and tissue sample (NP or B) in carbonate bicarbonate buffer (15 mmol L⁻¹, Na₂CO₃, 35 mmol L⁻¹, NaHCO₃, [pH 9.6]) for 24 h at 4 °C. Culture supernatant without any treatment was used as control. Each sample was independent and tested in triplicate. Blocking was performed by incubation with 6% fat-free milk in PBS-T (10 mM NaH₂PO₄, 150 mM NaCl, 0.005% Tween-20). After anti-SPCB-NF, (1:100) was added in 100 µL of PBS-T for 24 h at 4 °C. After that, the plate was incubated with Goat Anti-Rabbit IgG H&L conjugated horseradish peroxidase-labeled Cat#A16104, RRID:AB_2534776 (1:6000) in 100 µL of PBS-T. Three washes with PBS-T were given between each treatment. Enzymatic reaction was started by adding the substrate solution (0.5 mg de o-phenylenediamine per mL plus 0.01% H₂O₂ in 0.05 mmol L⁻¹ buffer de citratos [pH 5.2]). After 15 min, the reaction was stopped with 25 µL of 2.5 mmol L⁻¹ H₂SO₄ and the absorbance was measured at 490 nm in a microplate reader.

Immunoblot

5 µg of supernatant each group (control, 24 and 48 h NP, and 48 and 72 h B) was separated by SDS-PAGE (10%) and analyzed by immunoblot. In this, GAPDH was used as a loading control. Briefly, the separated proteins in polyacrylamide gel were transferred to a nitrocellulose membrane. The membrane was blocked with 10% fat-free milk at 4 °C for 24 h. Each sample was incubated with anti-SPCB-NF (1:100) in PBS-T. After 24 h incubation at 4 °C, samples were incubated with Goat Anti-Rabbit IgG conjugated horseradish peroxidase-labeled (1:1000) for 24 h at 4 °C. The protein recognition pattern was revealed by adding the substrate (4-chloro naphthol/methanol/H₂O₂). The reaction was stopped with PBS-T. To evaluate the differences between treatments, a densitometric analysis was performed using Image J software (RRID:SCR_003070).

Protease inhibitor toxicity and cell viability

The MTT assay was carried out to determine the mean effective concentration (EC₅₀) of pHMB or E64 after incubating trophozoites with each of these compounds. Briefly, one million *N. fowleri* trophozoites were placed in 96-well plates and incubated with different concentrations of pHMB (1, 5, 10 mM) or E64 (1, 5, 10, 20 µM). Treated trophozoites were incubated with 0.25 mg/mL MTT [3-(4,5-dimethylthiazol-2-yl)-2,5-diphenyltetrazolium bromide] in PBS for 4 h at

37 °C. Subsequently, 100 µL of DMSO (dimethylsulfoxide) was added for 20 min to solubilize the formazan crystals. The optical density was determined in a microplate reader at a wavelength of 540 nm. The EC₅₀ of pHMB and E64 was determined from the dose response curve in which the concentration of each inhibitor was plotted against the percentage of viability of the trophozoites after 30 min of treatment.

Once the EC₅₀ of pHMB (2.5 mM) and E64 (10 µM) was obtained, we evaluated the trophozoites viability after being incubated with each inhibitor by staining with trypan blue (which showed 99% viable trophozoites). Both EC₅₀ and cell viability after each treatment were evaluated in triplicate.

Survival

Five experimental groups with five mice each were intranasally infected with 12,000 live *N. fowleri* trophozoites preincubated with anti-SPCB-NF (1:100 or 1:250 dilution), p-hydroxymercuribenzoic acid 2.5 mM (pHMB), or L-trans-sepoxysuccinyl-leucylamide-4-guanidino-butane 10 µM (E64). Control group was infected with trophozoites without any treatment. All groups were monitored for 30 days. Once the symptoms related to meningitis (bristling hair, hunched or rigid body, and limited movement) appear in the mice, they are euthanized, and infection was confirmed by the recovery of trophozoites from brain sections under axenic conditions.

Statistical analysis

Data represent the mean ± SD of three independent assays. Multiple comparisons between control and problem groups were analyzed using a two-way ANOVA with $p < 0.05$. All analyses were carried out with the statistical program Prisma GraphPad v 7.00 (RRID:SCR_002798).

Results

Three-dimensional model and specificity of SPCB-NF and mRNA-probe of cathepsin B

The three-dimensional model ribbon representation of *N. fowleri* cathepsin B was performed by homology modeling using the crystal structure of rat procathepsin B, in which the amino acid sequence (corresponding to amino acids 71–94) selected for SPCB-NF was indicated in blue (Fig. 1a I, front view and II, back view).

The specificity of the selected peptide sequence was demonstrated by performing a phylogenetic analysis. The phylogenetic tree that was obtained from the multiple sequence alignment showed that the selected peptide has phylogenetic closeness with organisms of the same

genus (*N. gruberi*); however, no phylogenetic relationship was observed with other organisms, including mice and humans (Fig. 1a III). In addition, trophozoites-PMNs interactions were incubated with anti-SPCB-NF antibodies; however, no recognition was observed in PMNs (Fig. 1a IV), discarding the possibility of a cross-reaction between the peptide belonging to *N. fowleri* cathepsin B with neutrophil proteins.

Regarding the probe designed from the *N. fowleri* cathepsin B mRNA, the selected nucleotide sequence from which the probe was designed is shown in red (Fig. 1b I). The specificity of the selected probe was demonstrated by performing a phylogenetic analysis. This phylogenetic comparison showed that the only phylogenetic relationship was with *N. gruberi* (Fig. 1b II). On the other hand, when the probe was also incubated with trophozoites-PMNs, there was no signal in PMNs (Fig. 1b III). In this way, we also discard a possible probe nonspecific binding with nucleic acids of PMNs.

Presence of cathepsin B in *N. fowleri* trophozoites

Cathepsin B was detected in trophozoites interacted or not with PMN as well as in nasal cavity of mice infected with live trophozoites of *N. fowleri* (Fig. 2). Cathepsin B was localized at different sites of the amoeba (Fig. 2a red stain). Firstly, only some trophozoites non-interacted (Fig. 2a, upper panel, red stain) or interacted with PMNs (Fig. 2a, lower panel, red stain) showed the presence of this protein. In this way, the trophozoites that did not show staining are indicated with yellow boxes (Fig. 2a lower panel, phase contrast). Specifically in these results, it is worth to highlight that the cathepsin-B stain observed in trophozoites maintained in culture (non-interacted) was distributed punctually in cytoplasm (Fig. 2a upper merge, magnification image, white arrows), while the cathepsin-B stain in trophozoites interacted with PMNs was observed mainly in pseudopods and food-cups (Fig. 2a lower merge, magnification image, brown and yellow arrows, respectively). Once the presence of cathepsin

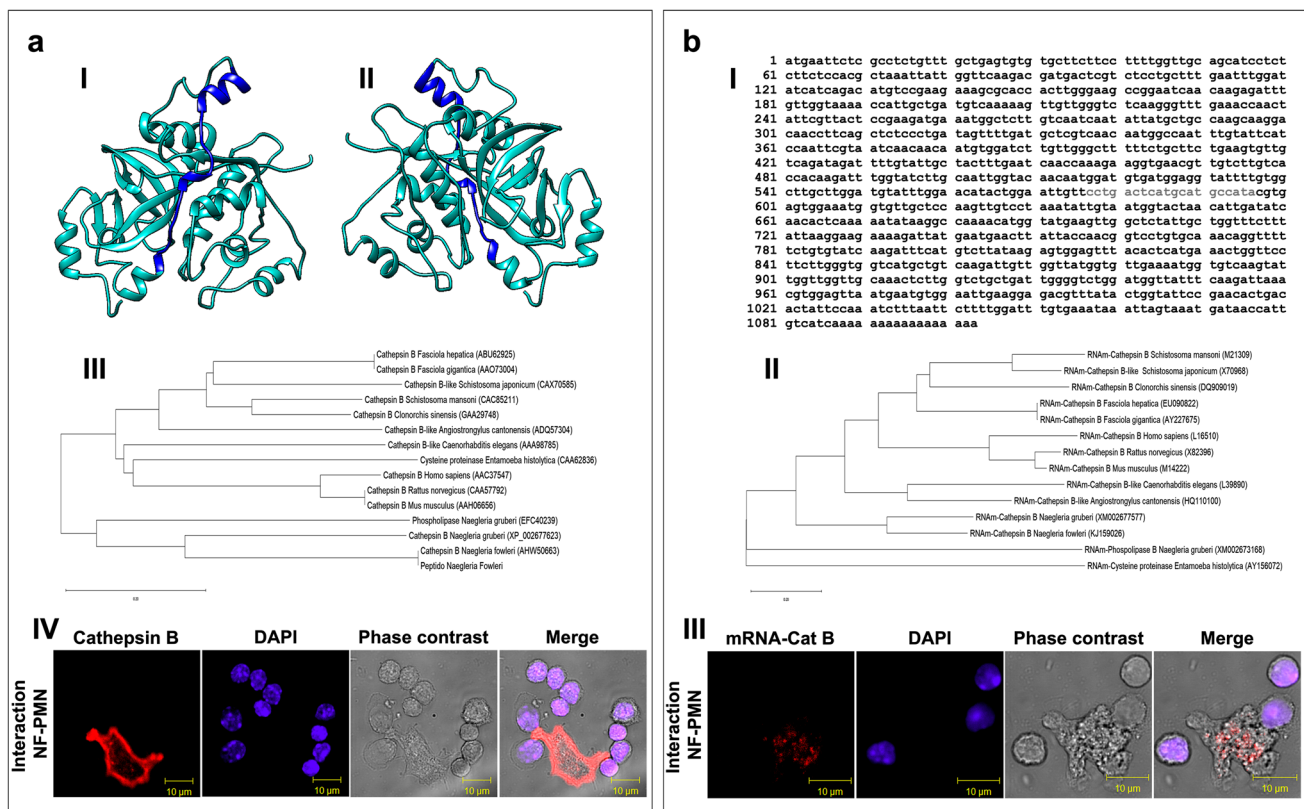


Fig. 1 Specificity tests of *N. fowleri* cathepsin B. **(a)** SPCB-NF specificity. Ribbon representation of three-dimensional model of *N. fowleri* cathepsin B by in silico design. **(I)** front view, **(II)** back view. Selected peptide is shown in blue (amino acids 71–94). **(III)** Phylogenetic comparison of amino acid sequence of cathepsin B from various organisms. **(IV)** Immunodetection of SPCB-NF (red stain) in mouse bone marrow PMNs interacted with *N. fowleri* trophozoites, in blue the DNA staining. **(b)** Probe specificity. **(I)** *N. fowleri* cathepsin B mRNA nucleotide sequence. Nucleotide sequence selected for probe design is shown in red (cDNA position 577–596). **(II)** Phylogenetic comparison of nucleotide sequence of cathepsin B mRNA from various organisms. **(III)** Detection of cathepsin B mRNA probe (red stain) in mouse bone marrow PMNs interacted with *N. fowleri* trophozoites in blue the DNA staining. Trees was constructed by neighbor-joining method

epsin B mRNA nucleotide sequence. Nucleotide sequence selected for probe design is shown in red (cDNA position 577–596). **(II)** Phylogenetic comparison of nucleotide sequence of cathepsin B mRNA from various organisms. **(III)** Detection of cathepsin B mRNA probe (red stain) in mouse bone marrow PMNs interacted with *N. fowleri* trophozoites in blue the DNA staining. Trees was constructed by neighbor-joining method

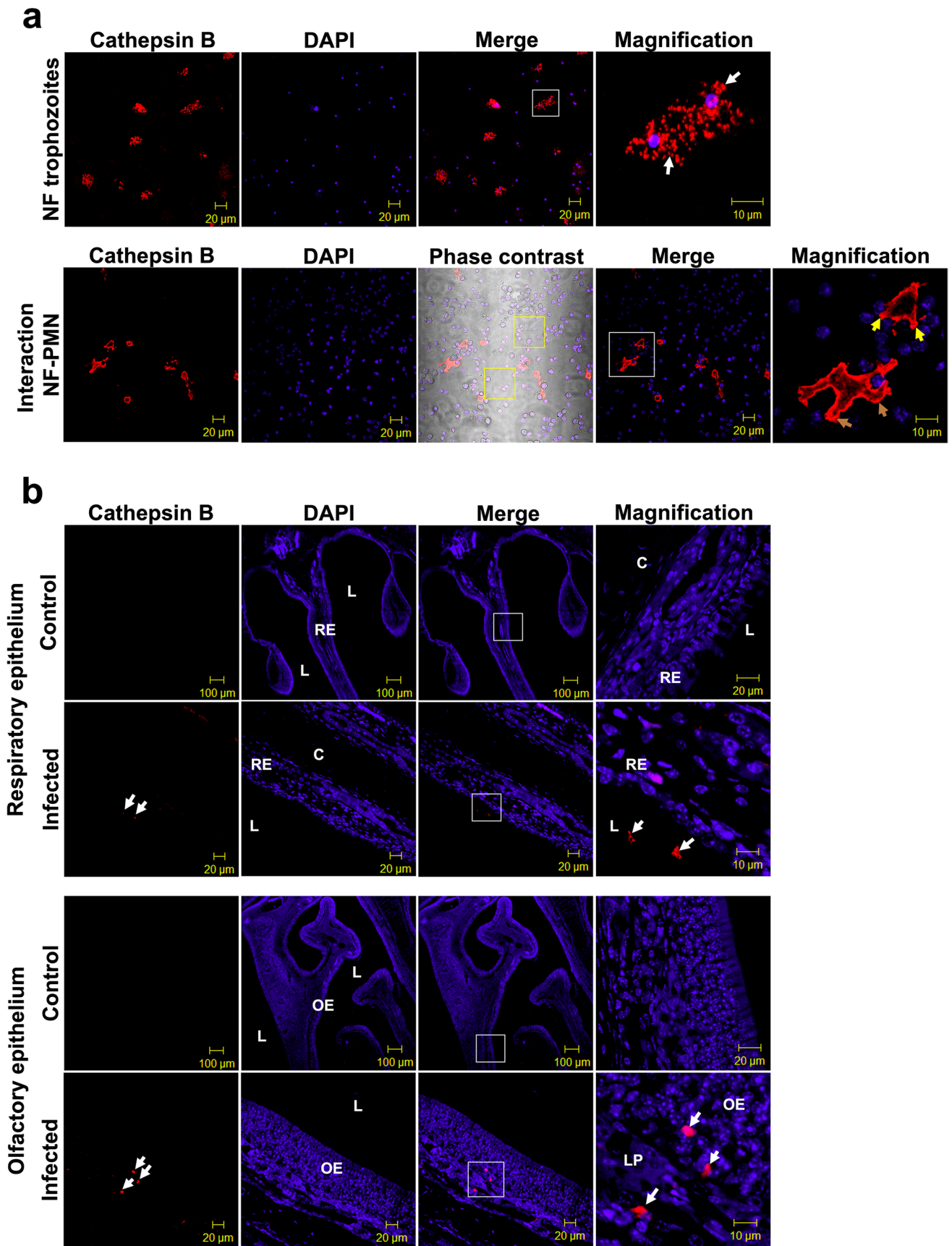


Fig. 2 Localization of cathepsin B in *N. fowleri* trophozoites (a) Immunodetection of cathepsin B in trophozoites alone or interacted with PMNs. Cathepsin B distribution in trophozoites alone was in cytoplasm (upper panel, white arrows), whereas trophozoite-PMNs interaction was in pseudopods and food-cups (lower panel, brown and yellow arrows, respectively). (b) Histological sections from uninfected and infected mice with *N. fowleri* trophozoites. Uninfected mice did not show cathepsin b staining in both the respiratory and olfactory epithelium (upper and lower panel control, respectively). On infected mice, trophozoites were in lumen before touching respiratory epithelial cells (upper panel infected, white arrows,) and migrating through olfactory epithelial cells (lower panel infected, white arrows). All of them with presence of cathepsin B. White boxes in merge represent area of magnification. Yellow boxes in phase contrast shown unstained trophozoites. L, lumen. C, cartilage. LP, lamina propria. RE, respiratory epithelium. OE, olfactory epithelium. Images are displayed at 40x (scale bar, 20 μ m) and 100x (scale bar, 10 μ m)

B in trophozoites was determined in vitro, we evaluated its presence in an in vivo infection model, for which Balb/c mice were infected with *N. fowleri* trophozoites and euthanized 24 h post-infection (Fig. 2b red stain, white arrows). DAPI was used to stain nuclei and allow visualization of epithelial nasal tissue structure (Fig. 2b blue stain). It is important to mention that both the respiratory epithelium (ER) and olfactory epithelium (OE) of the control groups (uninfected mice) did not show cathepsin B staining (Fig. 2b upper and lower panel control). Interestingly, in the group of infected mice, we identified trophozoites in the lumen before contacting RE which showed presence of cathepsin B (Fig. 2b, upper panel infected merge magnification, white arrows); the same cathepsin staining pattern of trophozoites was also located in OE, but unlike the trophozoites observed in the RE, these were found migrating through the epithelial cells and in lamina propria (Fig. 2b, lower panel infected merge magnification, white arrows).

Expression of cathepsin B-mRNA in *N. fowleri* trophozoites

In accordance with the in vitro results described above, we observed that depending on the stimulus to which *N. fowleri* trophozoites were subjected (with or without PMN), both the number of trophozoites and the distribution pattern of cathepsin B were different. In this way, we considered analyzing not only the protein but also the cathepsin-mRNA, which meant colocalization for both molecules, either in in vitro or in vivo experiments (Fig. 3). When trophozoites were kept in culture (Fig. 3a upper panels), there was expression of cathepsin-mRNA with the presence of cathepsin B (Fig. 3a red stain and green stain, respectively). Firstly, we can observe that cathepsin-mRNA was located mainly in nucleus and cytoplasm (Fig. 3a merge magnification, orange and turquoise arrows, respectively) while the presence of cathepsin B was more intense in pseudopods and food-cups (Fig. 3a merge magnification, brown and yellow arrows,

respectively) compared to cytoplasm where the stain was less intense.

When trophozoites were incubated with PMNs (Fig. 3a lower panels), following the same pattern of colors regarding cathepsin-mRNA in red and its protein in green, now we can observe that cathepsin-mRNA expression is shown outside of trophozoites contacting PMNs (pink arrows). Moreover, in some cases, the mRNA is not only in contact with PMNs but also is co-localized with the protein (gray arrows). These external structures might be debris amoebic as a result of the trophozoite integrity lost due to PMNs effect. On the other hand, cathepsin-mRNA expression was also observed in different areas within the cytoplasm of trophozoites (Fig. 3a merge magnification, turquoise arrow) as well as its protein which was in the membrane and cytoplasm (Fig. 3a merge magnification, brown and purple arrows, respectively).

When we evaluated the expression of mRNA at 24 h pos infection, stage considered as early during PAM model (Rojas-Hernández et al. 2004), we observed the presence of trophozoites which are located in the lumen of respiratory epithelium from infected mice (Fig. 3b). Some trophozoites expressed mRNA (red stain) as well as the cathepsin protein (green stain). In the merge image, clearly it is shown that the mRNA was mainly expressed in the trophozoite cytoplasm (turquoise arrow) while the protein is located in its membrane (white arrow). We provide phase-contrast images to enable the visualization of both trophozoites and cells that make up the respiratory epithelium.

Release of cathepsin B into extracellular medium

As we previously observed that cathepsin-mRNA was detected outside the trophozoites contacting PMNs and co-localized with the cathepsin protein in extracellular medium, we evaluate whether both *N. fowleri* molecules can be detected outside the trophozoites after interaction with PMNs either in vitro or in vivo (Fig. 4). Surprisingly, we corroborated that extracellular cathepsin-mRNA (Fig. 4a, red stain) was observed in contact with PMNs (turquoise arrow) and in some cases this molecule was also co-localized with cathepsin B (gray arrow), whereas the cathepsin protein (green stain) was observed in pseudopods (brown arrow) and food-cups (yellow arrow). It is worth mentioning that in this in vitro assay, the cathepsin-mRNA expression was not detected within amoeba.

After intranasal inoculation with trophozoites, these were located in the lumen of the nasal cavity (Fig. 4b), close to the respiratory epithelium cells. Trophozoites can be visualized through the protein and mRNA of cathepsin (green and red stain, respectively). For the protein distribution, we firstly observed a light stain in the cytoplasm of trophozoites (purple arrows). However, a more intense

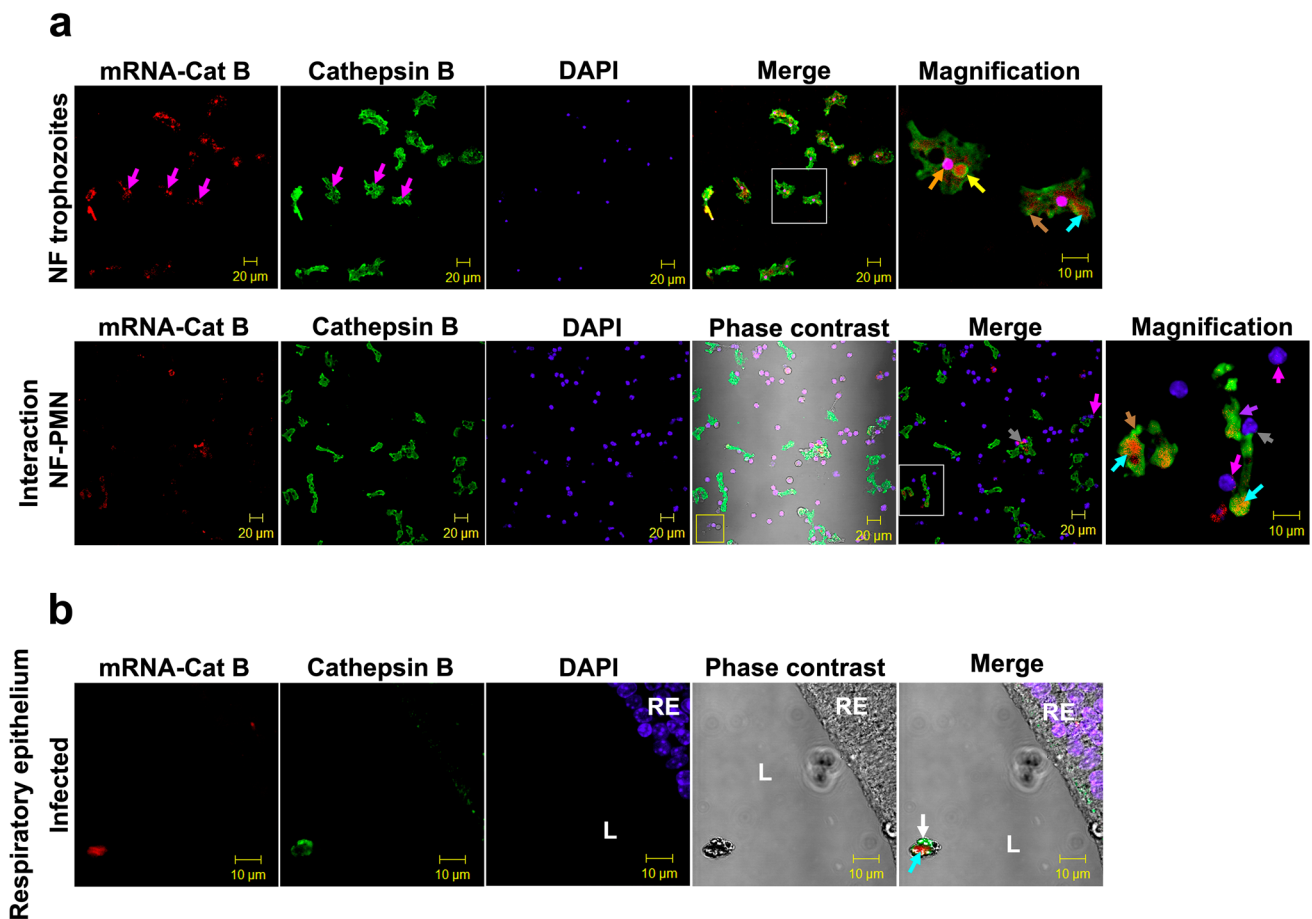


Fig. 3 Expression of cathepsin B mRNA in *N. fowleri* trophozoites (a) mRNA expression in trophozoites alone or interacted with PMNs. mRNA expression in trophozoites alone was in nucleus and cytoplasm (upper panel, orange and turquoise arrow, respectively) and protein was in pseudopods and food-cups (upper panel, brown and yellow arrows, respectively), whereas mRNA in trophozoite-PMNs interaction was in cytoplasm (lower panel, turquoise arrow) and protein was in membrane (lower panel, brown arrow). Under this treatment, mRNA was outside the trophozoites in contact with PMNs

alone (lower panel, pink arrows) or co-localized with protein (lower panel, gray arrows). (b) Histological sections from infected mice with *N. fowleri* trophozoites. Trophozoites were in lumen of nasal cavity of respiratory epithelium with mRNA expression and presence of cathepsin B (white and turquoise arrows, respectively). White boxes in merge represent area of magnification. Yellow boxes in phase contrast shown unstained trophozoites. L, lumen. RE, respiratory epithelium. Images are displayed at 40x (scale bar, 20 μ m) and 100x (scale bar, 10 μ m)

stain is detected in specific areas outside the amoeba (red arrows). Regarding the cathepsin-mRNA, it is observed in some cytoplasmic areas of the amoeba (turquoise arrows); specifically we can also observe that this molecule is distributed through some areas alike small vesicles inside the cytoplasm (blue arrows); apparently the mRNA is being transported to the place where the protein was released. All these events as well as the structures of both trophozoites and respiratory epithelium are better visualized in the magnification of the merge image (Fig. 4b).

The distribution of cathepsin mRNA (blue arrows) and its protein (white arrows) in *N. fowleri* is depicted at different levels that can be seen in greater detail on 3D images (Fig. 4c).

Release of Cathepsin B from *N. fowleri* during PAM

As we observed that *N. fowleri* trophozoites released cathepsin B during the PAM infection model, evidenced by positive staining outside the trophozoites (Fig. 4, green staining), now we carried out ELISA and immunoblot assays in order to confirm such release at 24, 48 or 72 h post-infection (Fig. 5). Amoebas from these infected groups were recovered from nasal passages and brain and their supernatants were recovered as it was described in Methodology section, while supernatant from control group was obtained from trophozoites that had been kept in culture for a year.

Amoebas from direct culture as well as those trophozoites isolated from brain and nasal passage at different times showed

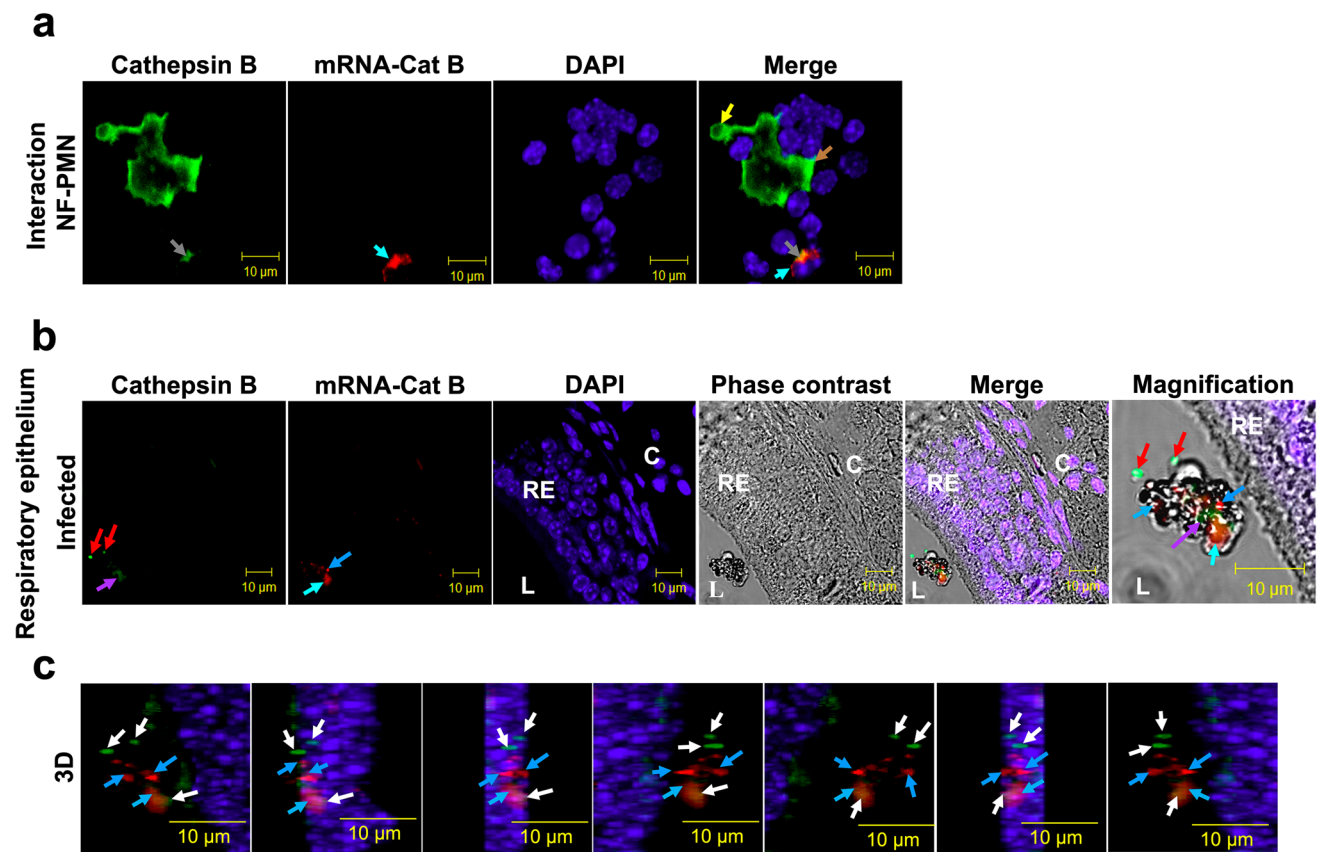


Fig. 4 Release of mRNA and protein into extracellular medium by *N. fowleri* trophozoites. **(a)** mRNA release by trophozoites interacted with PMNs was localized in contact with PMNs alone or co-localized with cathepsin B (turquoise and gray arrows, respectively), whereas protein was in pseudopodia or food-cups (brown and yellow arrows, respectively). **(b)** In tissue sections of infected mice, trophozoites expressed mRNA within small vesicles distributed in cytoplasm (blue

arrows), but their release could not be observed, whereas cathepsin B release was observed within small vesicles (red arrows). **(c)** mRNA and protein distribution shown in 3D images (blue and white arrows, respectively). All 3D images were taken from the magnification of figure b. L, lumen. C, cartilage. RE, respiratory epithelium. Images are displayed at 40x (scale bar, 20 µm) and 100x (scale bar, 10 µm)

release of cathepsin B into the extracellular medium (Fig. 5a). As we can observe, supernatants of amoeba culture recovered from nasal passages and brain showed a gradual increase in the release of this protein compared to control, being supernatants of culture amoebae from the brain (48, 72 h) that had the highest release of cathepsin B ($***p < 0.001$) followed by the culture recovered at 48 and 24 h from nasal passages ($**p < 0.01$ and $*p < 0.05$, respectively).

After confirming the release of cathepsin B into extracellular medium by ELISA assay, we identified the molecular weights corresponding to these released proteins of *N. fowleri* by immunoblot assay (Fig. 5b). Three bands of 26, 30, and 37 kDa were detected in all extracellular mediums, including the medium considered as control. Regarding the intensity of the bands, there was a similar pattern that those found in the ELISA results as the intensity of these bands was stronger in supernatants of trophozoite culture recovered from mice brains at 48 and 72 h after infection. Interestingly, the GAPDH loading control was inducible and its recognition and intensity was site and time dependent like cathepsin B.

In addition, one more band was observed in mice brain at 72 h after infection of approximately 250 kDa was observed only in supernatants of samples recovered from mice brain (72 h). Afterward, we determined if there were significant differences in recognition given by the anti-SPCB-NF to 26, 30, and 37 kDa protein bands through a densitometric analysis (Fig. 5c I, II, and III, respectively). Consistently, all groups showed significant differences compared to the control group ($*p < 0.05$, $**p < 0.01$ or $***p < 0.001$).

Cathepsin B inhibition

Finally, to determine cathepsin B role during *N. fowleri* infection, blocking assays were carried out where trophozoites were incubated with anti-SPCB-NF antibody at two dilutions (1:100 or 1:250) or with two protease inhibitors (pHMB or E64) before infecting the groups of mice (Fig. 6).

In mice infected with trophozoites pre-incubated with the anti-SPCB-NF antibody at dilutions of 1:100 or 1:250,

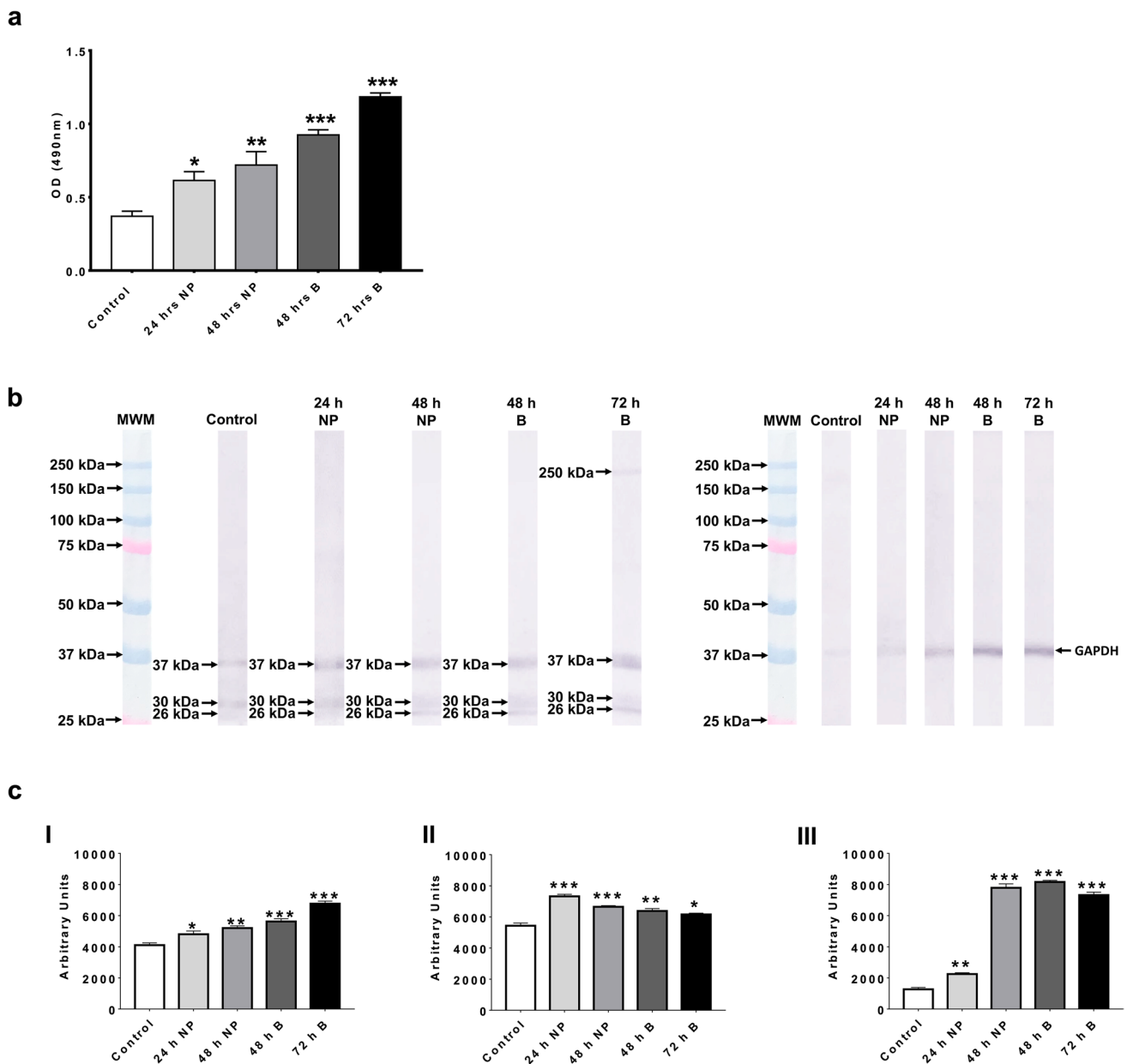


Fig. 5 Release of cathepsin B from *N. fowleri* during PAM. **(a)** Culture supernatants of amoebae recovered from nasal passages (NP) or brain (B) were evaluated for cathepsin B release. All treatments showed a significant increase compared to control of which culture supernatants of B recovered trophozoites showed the highest release. **(b)** Molecular weight analysis of secreted proteins. 26, 30 and 37 kDa were the most immunogenic bands recognized in all treatments.

GAPDH was used as a loading control. **(c)** Densitometric analysis of immunogenic bands evaluated with Image J software. (I) 37 kDa. (II) 30 kDa. (III) 26 kDa. All molecular weights evaluated by densitometry showed higher recognition in all treatments compared to the control. Significant differences versus control are indicated as follows: * $p < .05$, ** $p < .01$ or *** $p < .001$

we obtained 20% and 60% of survival, respectively. The period of died of mice that did not survive was within 11 to 21 days post-infection, whereas the mice that were infected with trophozoites without antibodies died within 5 to 9 days (Fig. 6a). When we analyzed the survival of infected mice with trophozoites pre-incubated with each inhibitor, we obtained 60% of survival with E-64. The period of died of

mice that did not survive was also extended up to 20–24 days post-infection. Interestingly, in mice infected with trophozoites pre-incubated with pHMB, we obtained a 100% of survival, whereas its control group also died within 5 to 9 days post-infection (Fig. 6b).

When we evaluated the distribution of cathepsin B, as well as its messenger in trophozoites preincubated with the

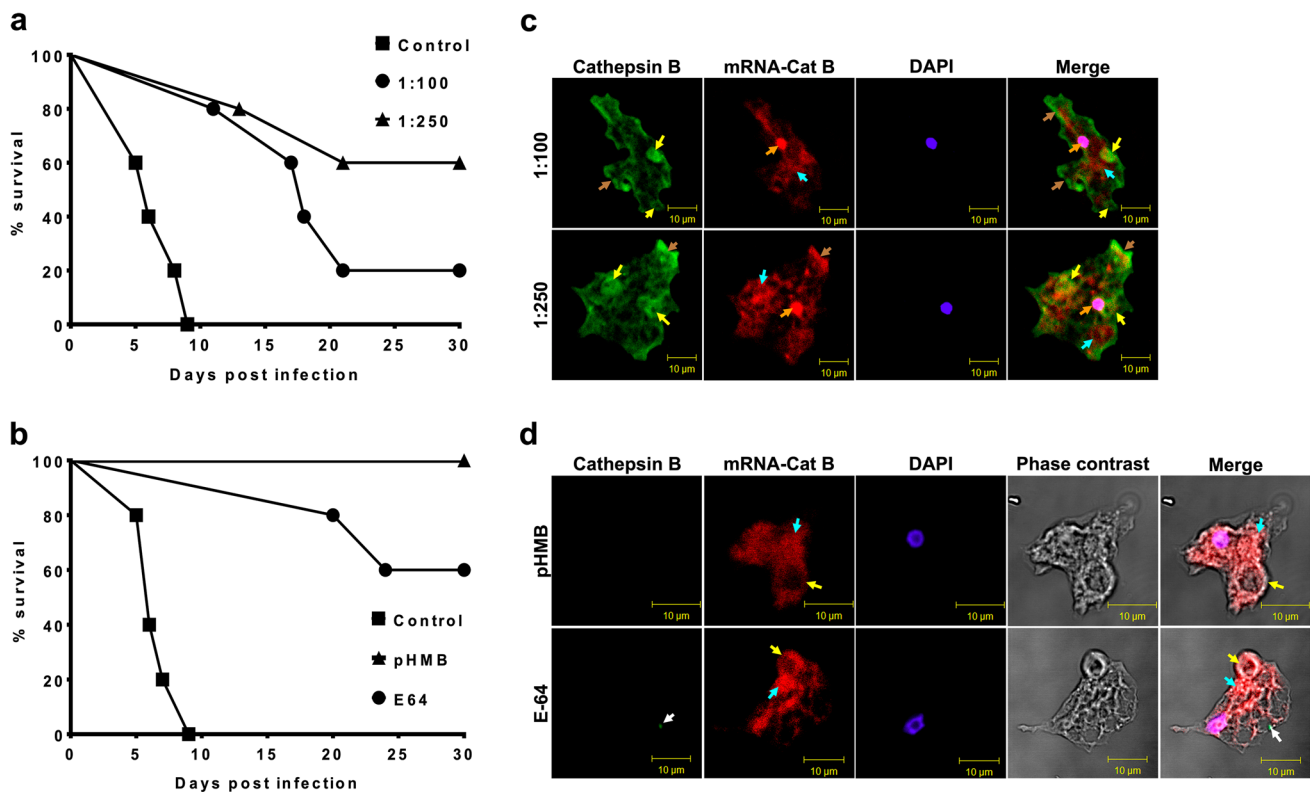


Fig. 6 Participation of *N. fowleri* cathepsin B during PAM. (a) Trophozoites preincubated with anti-SPCB-NF antibodies provided 20 and 60% survival (1:100 and 1:250 dilutions, respectively). (b) Trophozoites preincubated with pHMB provide 100% survival, whereas E-64, 60%. (c) Integrity of trophozoites pre-incubated with antibodies. In both antibody dilutions, cathepsin B distribution could be observed in pseudopods and food-cups (brown and yellow arrows,

respectively), whereas mRNA expression was in cytoplasm, nuclei, and pseudopods (turquoise, orange and brown arrows, respectively). (d) Integrity of trophozoites pre-incubated with pHMB or E-64. Cathepsin B could not be located under any treatment, but messenger was observed in food-cups and cytoplasm (yellow and turquoise arrows, respectively). Images are displayed at 100x (scale bar, 10 μ m)

anti-SPCB-NF antibody (Fig. 6c green and red stain, respectively), we observed that in both dilutions (1:100 and 1:250) the distribution of cathepsin B was mainly in food-cups and pseudopods (Fig. 6c, yellow and brown arrows, respectively) while messenger was located in nucleus and certain areas of the cytoplasm (Fig. 6c, orange and turquoise arrows, respectively). mRNA stain from trophozoites incubated at 1:250 with the antibody was also observed in a pseudopod (Fig. 6c, brown arrow). In the merge image, we observed the combination of each molecule (protein and mRNA) stained in different trophozoite structures.

When we evaluate the same molecules regarding their distribution, but now from trophozoites incubated with the inhibitors (pHMB or E-64), we clearly observed that cathepsin B was not detected in trophozoites incubated with pHMB inhibitor, whereas a lightly stain alike a small vesicle is observed when trophozoites were incubated with E-64 (Fig. 6d green stain and merge, both white arrows).

On the other hand, the mRNA was located in trophozoites treated with both inhibitors (Fig. 6d red stain), particularly the mRNA stain was located in food-cups (yellow arrows)

and cytoplasm (turquoise arrows). The distribution pattern for each molecule is better observed in the merge images for both inhibitors.

Discussion

In the present work, we evaluated the presence of cathepsin B protein as well as mRNA expression; in both cases we analyzed the distribution pattern within trophozoites of *N. fowleri* either in vitro or in vivo. In addition, this is the first time that the release of cathepsin B to the extracellular medium during different stages of the PAM is reported.

We determined the presence of cathepsin B in fixed trophozoites where we observed a punctual stain distributed throughout the cytoplasm.

In general, cathepsin B is the major representative of the CPs and is present in endosomal/lysosomal compartment of all types of cells under normal physiological conditions and is primarily involved in routine turnover of both intracellular and extracellular proteins, thus maintaining homeostatic

metabolic activity within cells where the acidic environment stimulates its activation (Kirschke et al. 1995; Hazen et al. 2000; Cavallo-Medved et al. 2011; Mort and Buttle 1997).

Here, we described that cathepsin B was distributed in several areas of the cytoplasm from trophozoites non-stimulated; however, when trophozoites were stimulated with PMNs, the protein predominated mainly in pseudopods and food-cups. Seong et al. (2017) also observed the locations of cathepsin B (NfCPB) and L (NfCPL) proteins in *N. fowleri* trophozoites non-stimulated using the same technique (immunocytochemistry assay). In this case, the proteins were detected with monoclonal antibodies (McAb) where both enzymes were in the cytoplasm, particularly in the pseudopodia and food-cup of the amoebas. The differences observed between the distribution of cathepsin B reported by Seong et al. (2017) where they located the protein in the membrane of non-stimulated trophozoites regarding our results, where we found it in the cytoplasm, might be to the specific conditions of the cultures such as the medium in which the trophozoites were kept, time between harvests (log phase of growth) or any other stimulus due to the manipulation of trophozoites before they were fixed.

Furthermore, we must highlight the difference with the antibodies used in the present work. We employed polyclonal peptide antibodies produced in rabbit where peptides used for immunization were evaluated with factors such as protein homology through phylogenetic analysis of the amino acid sequence of cathepsin B of different organisms and by using comparative modeling and molecular dynamics simulation (Fig. 1a). In general, peptide antibodies are usually of high specificity and affinity and have the advantage that the antigenic target is already well-defined (Trier et al. 2012, 2019). Their applications to multiple targets have emerged as powerful tools in research, diagnostics, vaccine development, and therapeutics (Trier et al. 2012). On the other hand, the reason why distribution of cathepsin B was localized mainly in membrane prolongations (pseudopods and food-cups) may be related to trophozoites defense against PMNs attack, since it has been suggested that cathepsins present on cell surface participating in pathogenesis (Betanzos et al. 2019; Lee et al. 2014). Particularly, it has been reported that the main functions of pseudopods include locomotion, cell communication, and nutrient uptake, while food-cups are involved to adhesion and trophocytosis (Allena 2013; Marciano-Cabral and Cabral 2007). The increased distribution of cathepsin B in the trophozoites membrane may be involved in surface modifications in response to the stimulus with PMNs, since we clearly observed a distribution change of cathepsin B in these trophozoites, unlike the stain observed in non-stimulated trophozoites, which was mainly in cytoplasm (Fig. 2). It has been described that cathepsin B is involved in plasma membrane retrieval, cell adhesion and signaling processes (Kos et al. 2009; Yadati et al. 2020).

Little is known about the molecular mechanisms used by *N. fowleri* to adhere and invade the host nasal epithelium; however, some studies in vitro have proposed that *N. fowleri* proteases including cathepsin B could be involved in these processes; for example: degrading mucins via a proteolytic mechanism (Cervantes-Sandoval et al. 2008; Martínez-Castillo et al. 2017), hydrolyzing several human proteins such as IgA, IgG, IgM, collagen, fibronectin, hemoglobin, and albumin (Lee et al. 2014), cleaving MDCK tight junction by degrading ZO-1 and claudin-1 (Shibayama et al. 2013) and extracellular matrix components (Vyas et al. 2015).

In the present study, we suggest that cathepsin B could be participating in such molecular mechanisms in an in vivo mouse model as we detected trophozoites positive for cathepsin B in the lumen of nasal cavity, close to apical region of epithelial cells, just before trophozoites contact respiratory epithelium and in lamina propria of olfactory epithelium (Fig. 2b). Here, cathepsin B would actively participate in adhesion and migration of trophozoites, favoring their access through different tissues.

We also located mRNA to cathepsin B predominantly in nucleus and cytoplasm of *N. fowleri* trophozoites kept in culture, probably being translated into protein to participate as a virulence mechanism. This is possible because *N. fowleri* cytoplasm presents various ribosomes either free along cytoplasm or associated with the membrane that form the rough endoplasmic reticulum (Martínez-Castillo et al. 2016), where this mRNA could be translated to protein cathepsin B in different sites of amoebae as we also observed in these trophozoites where the presence of this protein was evidenced in pseudopods and food-cups structures (Fig. 3a).

When trophozoites were incubated with PMNs, cathepsin-mRNA and its protein were observed not only in the membrane or cytoplasm but also outside of trophozoites contacting PMNs. It has recently been confirmed that mRNA can be released into extracellular medium in vesicles association or as RNA-protein complexes (Blenkiron et al. 2016; Ghosal 2018; Ghosal et al. 2015). Like cellular RNA, secreted RNA is thought to be involved in a variety of functions including defense, cell-to-cell communication, and altered behavior of nearby or distant cells (Blenkiron et al. 2016; Domenech et al. 2016; Ghosal et al. 2015; Koeppen et al. 2016).

In vivo, 24 h pos-infection we identified trophozoites expressing cathepsin B either in the lumen of RE or in EO epithelial cells. Interestingly, we found trophozoite cathepsin mRNA in vesicles distributed throughout cytoplasm apparently being transported to the site where cathepsin B will be secreted into small vesicles close to respiratory epithelial cells. Extracellular vesicles (EVs) can be released by different microorganisms such as bacteria, fungi, nematodes, and protozoa (de Souza and Barrias 2020; Wu et al. 2018). The content EVs can include lipids, proteins, or genetic

material (Wu et al. 2018). On the other hand, EVs can help microorganisms to interact with their environment, nutrient uptake, participate in infectious processes contributing to virulence factors release and immune response modulation, which favors their adaptation and survival in hostile environments (Gonçalves et al. 2018; Mantel and Marti 2014; Schwechheimer and Kuehn 2015). It has been reported that cathepsins are among the virulence factors released within EVs, which are related to the pathogenesis of different microorganisms (Dudley et al. 2008; Ocádiz et al. 2005; Schorey and Harding 2016) by participating in establishment, maintenance, and exacerbation of infection (McKerrow et al. 2006). This is probably one of the reasons why *N. fowleri* could be evading the immune response to favor its migration and establishment in the host. However, more in vivo studies must be carried out to determine the role of cathepsin B in PAM disease.

On the other hand, when we analyzed by ELISA and immunoblot assays the protein release at 24, 48 and 72 h post-infection, we found the presence of the enzyme mainly in the supernatants of trophozoites recovered from both nasal passages and brain. Apparently, cathepsin B release is progressively higher as the time after infection was increased. Although it is important to mention that at 24 and 72 h after inoculation, the amoebas could not be recovered from brain and nasal passages, respectively. With these results, we suggest that cathepsin B could be participating in the initial stages of the infection contributing to the trophozoites adhesion and migration from the nasal cavity to the brain as well as in the tissue destruction. Surprisingly, the GAPDH loading control showed a recognition pattern similar to that observed with cathepsin B. GAPDH is a housekeeping enzyme considered as inducible proteins which are present ubiquitously in most living beings. In addition to performing essential metabolic functions, housekeeping enzymes participate in pathogenesis enhancing virulence in many pathogens. On the other hand, contact of pathogens with host cells has been reported to result in the secretion of pathogen GAPDH. Together the above makes them targets for the development of new strategies to control the infection (Pancholi and Chhatwal 2003).

Although tissue damage has not been reported in early stages of PAM (Jarolim et al. 2000; John 1982; Martinez et al. 1973; Rojas-Hernández et al. 2004), it is known that *N. fowleri* has mucin-degrading proteases, elastases, lipases, hydrolases, and phospholipases which could favor their survival and adhesion to nasal epithelium together PAM development (Martínez-Castillo et al. 2017; Güémez and García 2021).

During trophozoite migration to the brain, it has been proposed that they probably degrade tight junction components such as Claudin-1 and ZO-1 (Shibayama et al. 2013) gaining access through extracellular matrix (Marciano-Cabral and Cabral 2007) through fibronectin and collagen degradation

(Siddiqui et al. 2016; Vyas et al. 2015). Finally, these proteases have also been related to nerve cells destruction or nutrient uptake (Klemba and Goldberg 2002; Marciano-Cabral and Cabral 2007; Martínez-Castillo et al. 2015). We clearly observed in our experiments of ELISA and immunoblot that cathepsin B is release into extracellular medium with a significant increase when trophozoites reached the brain.

Specifically, by immunoblot we observed that 37-, 30-, and 26-kDa bands were recognized in all groups evaluated. For 37 kDa band, it has been reported with mucinolytic activity which can be inhibited by CPs inhibitors. Thus, it has been associated with the evasion of host immune response (Cervantes-Sandoval et al. 2008; Martínez-Castillo et al. 2016). Moreover, it has been considered as an immunogenic polypeptide band (Rojas-Hernández et al. 2020). Regarding to the 30 kDa band, it has been considered as a CP which is secreted and degrades components of extracellular matrix (Aldape et al. 1994; Siddiqui et al. 2016; Piña-Vázquez et al. 2012). For 26 kDa band, it has been reported as a part of membrane protein profile of *N. fowleri* (Flores-Huerta et al. 2020).

Other band found in this work was 250 kDa, band that was observed in supernatants of trophozoites recovered from mice tissue. Here we describe some characteristics that have been attributed to this protein band. The 250-kDa band has been considered with mucinolytic activity and capable of degrading collagen (Chávez-Munguía et al. 2014; Martínez-Castillo et al. 2016); in addition, immunogenic properties have been attributed to this polypeptide band capable to provide 80% protection in mice immunized and challenged with lethal dose of *N. fowleri* trophozoites (Castillo-Ramírez et al. 2021; Rojas-Hernández et al. 2020). The fact that our antibody recognized different bands does not represent the lack of specificity of our antibody. The specificity of antibodies is their ability to recognize and bind to their target epitope. However, recognition of different bands may represent degradation of proteins, proteins containing the target epitope, or cleavages of post-translational modifications (Pillai-Kastoori et al. 2020).

We found that trophozoites preincubated with antibodies or two different inhibitors, pHMB or E-64, decreased the mortality of infected mice. Anti- SPCB-NF antibodies are probably inhibiting *N. fowleri* adhesion to nasal epithelium of mice. In a similar study, García-Rivera et al. (1999) pre-incubated *E. histolytica* trophozoites with antibodies directed against EhCP112 CP and found that these antibodies inhibit trophozoites adhesion to erythrocytes or epithelial cells. Campos-Rodríguez et al. (2004) observed that when *Acanthamoeba polyphaga* is incubated with antibodies purified from colostrum of healthy women, these antibodies can inhibit adhesion of these amoebae to canine kidney

cells (MDCK), whereas Fiori et al. (1997) observed that the incubation of *T. vaginalis* with antibodies directed against 65 kDa CP reduces cytotoxicity in HeLa cells. In our work, we observed at two different dilutions of our antibody, it is obtained between 20 and 60% of survival. Clearly, we suggest that cathepsin B participates during *N. fowleri* infection, although future studies would need to determine the exact role of this antibody anti-cathepsin to avoid the *N. fowleri* adhesion process to epithelium. On the other hand, we also observed that both E-64 and PHMB inhibitors increased the survival from infected mice with trophozoites pre-incubated with these inhibitors up to 60 and 100%, respectively.

Aldape et al. (1994) previously had reported that E-64 completely inhibited protease activity at 1 μ M in *N. fowleri* trophozoites; thus, the degradation of the extracellular matrix from R22 cells (derived from rat vascular smooth muscle) was also inhibited. Moreover, E-64 caused decrease in the activity of *N. fowleri* on the cytopathic effect of baby hamster kidney cells (BHK). Martínez-Castillo et al. (2017) demonstrated that E-64 partially inhibits the 94 kDa protein with mucinolytic activity, blocking the cell damage of mucoepithelial cells (NCI-H292) caused by *N. fowleri*. Finally, these authors showed that pHMB was capable of totally blocking mucinolytic activity of the proteases secreted by *N. fowleri*.

The differences in the inhibitory effect of pHMB compared to E-64 may be due to the number of substrates related to each inhibitor. It is known that within the substrates related to pHMB are CPs (cathepsins B, C, F, H, K, L, O, S, V, X, and W), but also some serine proteases and metalloproteases that have groups thiol while E-64 is a specific inhibitor of CPs which include cathepsins B, H, and L. (Bartlett and Brown 1990; Wadhawan et al. 2014).

On the other hand, E64 is not able to effectively penetrate the membrane (Wilcox and Mason 1992) although it can be taken up by pinocytosis acting mainly against surface-bound CPs or against proteins within phagolysosomes but may be less effective against CPs activated at other sites inside or outside cells. Nowak et al. (2004) reported that *E. histolytica* is capable of developing resistance to the effect caused by E64 and this resistance is associated with the secretion of pro-enzymes which can be activated in extracellular medium. On the other hand, although some mechanisms responsible for drug resistance in protozoan parasites have been identified (Borst and Ouellette 1995; Cowman 1995; Pérez-Victoria et al. 2002) including decreased influx or acceleration of drug egress the specific processes by which E64 is eliminated are unclear. Finally, the morphology of *N. fowleri* trophozoites after being incubated with E64 showed the appearance of a network of fibril-like structures distributed throughout the cytoplasm, which could reflect loss of

shape in the trophozoites morphology as we can clearly see in Fig. 6d. These changes in cytoplasm of *N. fowleri* trophozoite probably reduce its ability to adhere to the nasal epithelium of mice and therefore the infection.

N. fowleri shows great activity in synthesis and presence of cathepsin B because it was found in cytoplasm and membrane, in addition to the fact that both the messenger and protein can be released into the extracellular medium. All the above suggest that this enzyme actively participates in metabolism, nutrient uptake, and as a virulence factor during *N. fowleri* infection. Finally, as they are considered highly immunogenic proteins, their inhibition caused high survival rates, which makes them important targets for the development of drugs or vaccines.

Acknowledgements The study was funded by the following grants: CONACyT 265230 and IPN-SIP 20221248.

Authors' contributions **Conceptualization** was performed by Saúl Rojas-Hernández, María Maricela Carrasco-Yépez, and Itzel Berenice Rodríguez-Mera. **Data curation** was carried out by Itzel Berenice Rodríguez-Mera, Diego Arturo Castillo-Ramírez, Ismael Vásquez-Moctezuma, Gema Ramírez-Salinas, José Correa-Basurto and Erika Rosales-Cruz. **Formal analysis** was performed by Saúl Rojas-Hernández, María Maricela Carrasco-Yépez, Itzel Berenice Rodríguez-Mera and Diego Arturo Castillo-Ramírez. **Funding acquisition** was carried out by Saúl Rojas-Hernández and María Maricela Carrasco-Yépez. **Investigation**: Saúl Rojas-Hernández, María Maricela Carrasco-Yépez, Itzel Berenice Rodríguez-Mera, Diego Arturo Castillo-Ramírez, Ismael Vásquez-Moctezuma, Gema Ramírez-Salinas, José Correa-Basurto and Erika Rosales-Cruz. **Project administration and resources** were performed by Saúl Rojas-Hernández and María Maricela Carrasco-Yépez. **Validation**: Saúl Rojas-Hernández, María Maricela Carrasco-Yépez, Itzel Berenice Rodríguez-Mera, Diego Arturo Castillo-Ramírez, Ismael Vásquez-Moctezuma, Gema Ramírez-Salinas, José Correa-Basurto and Erika Rosales-Cruz. **Visualization** was carried out by Saúl Rojas-Hernández, María Maricela Carrasco-Yépez, and Itzel Berenice Rodríguez-Mera. **Writing—original draft**—was performed by Saúl Rojas-Hernández, María Maricela Carrasco-Yépez, and Itzel Berenice Rodríguez-Mera. **Writing—review and editing**—was performed by Saúl Rojas-Hernández, María Maricela Carrasco-Yépez, and Itzel Berenice Rodríguez-Mera.

Data availability All data generated or analyzed during this study are included in this manuscript.

Declarations

Ethical approval This study was conducted in accordance with the Mexican federal regulations for animal experimentation and care (ESM, CICAL-ADDEM-05/27–09-2019, NOM-062-ZOO-1999, Ministry of Agriculture, Mexico City, Mexico).

Consent to participate and publication All authors are aware of their participation in this manuscript and agree to its publication.

Conflict of interest The authors declare that they have no conflict of interest.

References

- Aldape K, Huizinga H, Bouvier J, McKerrow J (1994) *Naegleria fowleri*: characterization of a secreted histolytic cysteine protease. *Exp Parasitol* 78(2):230–241. <https://doi.org/10.1006/expr.1994.1023>
- Allena R (2013) Cell migration with multiple pseudopodia: temporal and spatial sensing models. *Bull Math Biol* 75(2):288–316. <https://doi.org/10.1007/s11538-012-9806-1>
- Aurongzeb M et al (2021) In silico analysis of *Naegleria fowleri* cathepsin B paralogs: important drug targets. *Eur Rev Med Pharmacol sci* 25(8):3162–3172. https://doi.org/10.26355/eurrev_202104_25725
- Barrett AJ, Brown MA (1990) Chicken liver Pz-peptidase, a thiol-dependent metallo-endopeptidase. *Biochem J* 271(3):701–706. <https://doi.org/10.1042/bj2710701>
- Betanzos A, Bañuelos C, Orozco E (2019) Host Invasion by Pathogenic Amoebae: Epithelial Disruption by Parasite Proteins. *Genes* 10(8). <https://doi.org/10.3390/genes10080618>
- Blenkiron C et al (2016) Uropathogenic *Escherichia coli* Releases Extracellular Vesicles That Are Associated with RNA. *PLoS ONE* 11(8):e0160440. <https://doi.org/10.1371/journal.pone.0160440>
- Borst P, Ouellette M (1995) New mechanisms of drug resistance in parasitic protozoa. *Annu Rev Microbiol* 49:427–460. <https://doi.org/10.1146/annurev.mi.49.100195.002235>
- Campos-Rodríguez R et al (2004) Human IgA inhibits adherence of *Acanthamoeba polyphaga* to epithelial cells and contact lenses. *Can J Microbiol* 50(9):711–718. <https://doi.org/10.1139/w04-057>
- Carrasco-Yepez M et al (2013) *Naegleria fowleri* glycoconjugates with residues of α -D-mannose are involved in adherence of trophozoites to mouse nasal mucosa. *Parasitol Res* 112(10):3615–3625. <https://doi.org/10.1007/s00436-013-3549-2>
- Carrasco-Yepez MM et al (2019) Mouse neutrophils release extracellular traps in response to *Naegleria fowleri*. *Parasite Immunol* 41(2):e12610. <https://doi.org/10.1111/pim.12610>
- Castillo-Ramírez DA, Carrasco-Yépez MM, Rodríguez-Mera IB, Reséndiz-Albor AA, Rosales-Cruz É, Rojas-Hernández S (2021) A 250-kDa glycoprotein of *Naegleria fowleri* induces protection and modifies the expression of α 4 β 1 and LFA-1 on T and B lymphocytes in mouse meningitis model. *Parasite Immunol* 43(12):e12882. <https://doi.org/10.1111/pim.12882>
- Cavallo-Medved D, Moin K, Sloane B (2011) Cathepsin B: Basis Sequence: Mouse. *The AFCS-Nature Molecule Pages* 2011:A000508
- Cervantes-Sandoval I, Serrano-Luna JJ, García-Latorre E, Tsutsumi V, Shibayama M (2008) Mucins in the host defence against *Naegleria fowleri* and mucinolytic activity as a possible means of evasion. *Microbiology* (reading, England) 154(Pt 12):3895–3904. <https://doi.org/10.1099/mic.0.2008/019380-0>
- Chávez-Munguía B, Villatoro LS, Omaña-Molina M, Rodríguez-Monroy MA, Segovia-Gamboa N, Martínez-Palomo A (2014) *Naegleria fowleri*: contact-dependent secretion of electron-dense granules (EDG). *Exp Parasitol* 142:1–6. <https://doi.org/10.1016/j.exppara.2014.03.027>
- Cowman AF (1995) Mechanisms of drug resistance in malaria. *Aust N Z J Med* 25(6):837–844. <https://doi.org/10.1111/j.1445-5994.1995.tb02889.x>
- de Souza W, Barrias ES (2020) Membrane-bound extracellular vesicles secreted by parasitic protozoa: cellular structures involved in the communication between cells. *Parasitol Res* 119(7):2005–2023. <https://doi.org/10.1007/s00436-020-06691-7>
- Domenech M, Pedrero-Vega E, Prieto A, García E (2016) Evidence of the presence of nucleic acids and β -glucan in the matrix of non-typeable *Haemophilus influenzae* in vitro biofilms. *Sci Rep* 6:36424. <https://doi.org/10.1038/srep36424>
- Dudley R, Alsam S, Khan NA (2008) The role of proteases in the differentiation of *Acanthamoeba castellanii*. *FEMS Microbiol Lett* 286(1):9–15. <https://doi.org/10.1111/j.1574-6968.2008.01249.x>
- Fiori PL, Rappelli P, Addis MF, Mannu F, Cappuccinelli P (1997) Contact-dependent disruption of the host cell membrane skeleton induced by *Trichomonas vaginalis*. *Infect Immun* 65(12):5142–5148. <https://doi.org/10.1128/iai.65.12.5142-5148.1997>
- Flores-Huerta N et al (2020) A comparative study of the membrane proteins from *Naegleria* species: A 23-kDa protein participates in the virulence of *Naegleria fowleri*. *Eur J Protistol* 72:125640. <https://doi.org/10.1016/j.ejop.2019.125640>
- García-Rivera G, Rodríguez MA, Ocadíz R, Martínez-López MC, Arroyo R, González-Robles A, Orozco E (1999) Entamoeba histolytica: a novel cysteine protease and an adhesin form the 112 kDa surface protein. *Mol Microbiol* 33(3):556–568. <https://doi.org/10.1046/j.1365-2958.1999.01500.x>
- Ghosal A et al (2015) The extracellular RNA complement of *Escherichia coli*. *MicrobiologyOpen* 4(2):252–266. <https://doi.org/10.1002/mbo3.235>
- Ghosal A (2018) Secreted bacterial RNA: an unexplored avenue. *FEMS microbiology letters* 365(7). <https://doi.org/10.1093/femsle/fny036>
- Gonçalves DS et al (2018) Extracellular vesicles and vesicle-free secretome of the protozoa *Acanthamoeba castellanii* under homeostasis and nutritional stress and their damaging potential to host cells. *Virulence* 9(1):818–836. <https://doi.org/10.1080/21505594.2018.1451184>
- Grace E, Asbill S, Virga K (2015) *Naegleria fowleri*: pathogenesis, diagnosis, and treatment options. *Antimicrob Agents Chemother* 59(11):6677–6681. <https://doi.org/10.1128/aac.01293-15>
- Güémez A, García E (2021) Primary Amoebic Meningoencephalitis by *Naegleria fowleri*: Pathogenesis and Treatments. *Biomolecules* 11(9). <https://doi.org/10.3390/biom11091320>
- Han KL, Lee HJ, Shin MH, Shin HJ, Im KI, Park SJ (2004) The involvement of an integrin-like protein and protein kinase C in amoebic adhesion to fibronectin and amoebic cytotoxicity. *Parasitol Res* 94(1):53–60. <https://doi.org/10.1007/s00436-004-1158-9>
- Hazen LG et al (2000) Comparative localization of cathepsin B protein and activity in colorectal cancer. *J Histochem Cytochem: Off J Histochem Soc* 48(10):1421–1430. <https://doi.org/10.1177/002215540004801012>
- Jahangeer M et al (2020) *Naegleria fowleri*: Sources of infection, pathophysiology, diagnosis, and management; a review. *Clin Exp Pharmacol Physiol* 47(2):199–212. <https://doi.org/10.1111/1440-1681.13192>
- Jamerson M, da Rocha-Azevedo B, Cabral GA, Marciano-Cabral F (2012) Pathogenic *Naegleria fowleri* and non-pathogenic *Naegleria lovaniensis* exhibit differential adhesion to, and invasion of, extracellular matrix proteins. *Microbiology* (reading, England) 158(Pt 3):791–803. <https://doi.org/10.1099/mic.0.055020-0>
- Jaroli KL, McCosh JK, Howard MJ (2002) The role of blood vessels and lungs in the dissemination of *Naegleria fowleri* following intranasal inoculation in mice. *Folia parasitologica* 49(3):183–8. <https://doi.org/10.14411/fp.2002.035>
- Jarolim KL, McCosh JK, Howard MJ, John DT (2000) A light microscopy study of the migration of *Naegleria fowleri* from the nasal submucosa to the central nervous system during the early stage of primary amoebic meningoencephalitis in mice. *J Parasitol* 86(1):50–55. [https://doi.org/10.1645/0022-3395\(2000\)086\[0050:Almsot\]2.0.Co;2](https://doi.org/10.1645/0022-3395(2000)086[0050:Almsot]2.0.Co;2)
- Jeong SR, Kang SY, Lee SC, Song KJ, Im KI, Shin HJ (2004) Decreasing effect of an anti-NfaI polyclonal antibody on the in vitro cytotoxicity of pathogenic *Naegleria fowleri*. *Korean J Parasitol* 42(1):35–40. <https://doi.org/10.3347/kjp.2004.42.1.35>

- John DT (1982) Primary amebic meningoencephalitis and the biology of *Naegleria fowleri*. *Annu Rev Microbiol* 36:101–123. <https://doi.org/10.1146/annurev.mi.36.100182.000533>
- Kim JH, Yang AH, Sohn HJ, Kim D, Song KJ, Shin HJ (2009) Immunodominant antigens in *Naegleria fowleri* excretory–secretory proteins were potential pathogenic factors. *Parasitol Res* 105(6):1675–1681. <https://doi.org/10.1007/s00436-009-1610-y>
- Kirschke H, Barrett AJ, Rawlings ND (1995) Proteinases 1: lysosomal cysteine proteinases. *Protein Profile* 2(14):1581–1643
- Klemba M, Goldberg DE (2002) Biological roles of proteases in parasitic protozoa. *Annu Rev Biochem* 71:275–305. <https://doi.org/10.1146/annurev.biochem.71.090501.145453>
- Koepfen K et al (2016) A Novel Mechanism of Host-Pathogen Interaction through sRNA in Bacterial Outer Membrane Vesicles. *PLoS Pathog* 12(6):e1005672. <https://doi.org/10.1371/journal.ppat.1005672>
- Kos J, Jevnikar Z, Obermajer N (2009) The role of cathepsin X in cell signaling. *Cell Adh Migr* 3(2):164–166. <https://doi.org/10.4161/cam.3.2.7403>
- Lee J et al (2014) Novel cathepsin B and cathepsin B-like cysteine protease of *Naegleria fowleri* excretory-secretory proteins and their biochemical properties. *Parasitol Res* 113(8):2765–2776. <https://doi.org/10.1007/s00436-014-3936-3>
- Loyola PK et al (2013) Theoretical analysis of the neuraminidase epitope of the Mexican A H1N1 influenza strain, and experimental studies on its interaction with rabbit and human hosts. *Immunol Res* 56(1):44–60. <https://doi.org/10.1007/s12026-013-8385-z>
- Mantel PY, Marti M (2014) The role of extracellular vesicles in *Plasmodium* and other protozoan parasites. *Cell Microbiol* 16(3):344–354. <https://doi.org/10.1111/cmi.12259>
- Marciano-Cabral F, Cabral GA (2007) The immune response to *Naegleria fowleri* amoebae and pathogenesis of infection. *FEMS Immunol Med Microbiol* 51(2):243–259. <https://doi.org/10.1111/j.1574-695X.2007.00332.x>
- Martínez J, Duma RJ, Nelson EC, Moretta FL (1973) Experimental naegleria meningoencephalitis in mice. Penetration of the olfactory mucosal epithelium by *Naegleria* and pathologic changes produced: a light and electron microscope study. *Lab Investigation J Tech Methods Pathol* 29(2):121–33
- Martínez-Castillo M, Ramírez-Rico G, Serrano-Luna J, Shibayama M (2015) Iron-Binding Protein Degradation by Cysteine Proteases of *Naegleria fowleri*. *Biomed Res Int* 2015:416712. <https://doi.org/10.1155/2015/416712>
- Martínez-Castillo M, Cárdenas-Zúñiga R, Coronado-Velázquez D, Debnath A, Serrano-Luna J, Shibayama M (2016) *Naegleria fowleri* after 50 years: is it a neglected pathogen? *J Med Microbiol* 65(9):885–896. <https://doi.org/10.1099/jmm.0.000303>
- Martínez-Castillo M et al (2017) Nf-GH, a glycosidase secreted by *Naegleria fowleri*, causes mucin degradation: an in vitro and in vivo study. *Future Microbiol* 12(9):781–799. <https://doi.org/10.2217/fmb-2016-0230>
- Mat Amin N (2004) Proteinases in *Naegleria fowleri* (strain NF3), a pathogenic amoeba: a preliminary study. *Trop Biomed* 21(2):57–60
- McKerrow JH, Caffrey C, Kelly B (2006) Loke Pn, Sajid MJARPM. Proteases in Parasitic Dis 1:497–536
- Mishra BB, Gundra UM, Teale JM (2009) Toll-like receptors in CNS parasitic infections. *Curr Top Microbiol Immunol* 336:83–104. https://doi.org/10.1007/978-3-642-00549-7_5
- Mort JS, Buttle DJ (1997) Cathepsin B. *Int J Biochem Cell Biol* 29(5):715–720. [https://doi.org/10.1016/S1357-2725\(96\)00152-5](https://doi.org/10.1016/S1357-2725(96)00152-5)
- Moseman EA (2020) Battling brain-eating amoeba: Enigmas surrounding immunity to *Naegleria fowleri*. *PLoS Pathog* 16(4):e1008406. <https://doi.org/10.1371/journal.ppat.1008406>
- Nowak N, Lotter H, Tannich E, Bruchhaus I (2004) Resistance of *Entamoeba histolytica* to the cysteine proteinase inhibitor E64 is associated with secretion of pro-enzymes and reduced pathogenicity. *J Biol Chem* 279(37):38260–38266. <https://doi.org/10.1074/jbc.M405308200>
- Ocádiz R et al (2005) EhCP112 is an *Entamoeba histolytica* secreted cysteine protease that may be involved in the parasite-virulence. *Cell Microbiol* 7(2):221–232. <https://doi.org/10.1111/j.1462-5822.2004.00453.x>
- Pancholi V, Chhatwal GS (2003) Housekeeping enzymes as virulence factors for pathogens. *Int J Med Microbiol: IJMM* 293(6):391–401. <https://doi.org/10.1078/1438-4221-00283>
- Pérez-Victoria JM, Di Pietro A, Barron D, Ravelo AG, Castanys S, Gamarro F (2002) Multidrug resistance phenotype mediated by the P-glycoprotein-like transporter in *Leishmania*: a search for reversal agents. *Curr Drug Targets* 3(4):311–333. <https://doi.org/10.2174/1389450023347588>
- Pillai-Kastoori L et al (2020) Antibody validation for Western blot: By the user, for the user. *J Biol Chem* 295(4):926–939. <https://doi.org/10.1074/jbc.RA119.010472>
- Piña-Vázquez C, Reyes-López M, Ortiz-Estrada G, de la Garza M, Serrano-Luna J (2012) Host-parasite interaction: parasite-derived and -induced proteases that degrade human extracellular matrix. *J Parasitol Res* 2012:748206. <https://doi.org/10.1155/2012/748206>
- Pugh JJ, Levy RA (2016) *Naegleria fowleri*: Diagnosis, Pathophysiology of Brain Inflammation, and Antimicrobial Treatments. *ACS Chem Neurosci* 7(9):1178–1179. <https://doi.org/10.1021/acschemneuro.6b00232>
- Rojas-Hernández S, Jarillo-Luna A, Rodríguez-Monroy M, Moreno-Fierros L, Campos-Rodríguez R (2004) Immunohistochemical characterization of the initial stages of *Naegleria fowleri* meningoencephalitis in mice. *Parasitol Res* 94(1):31–36. <https://doi.org/10.1007/s00436-004-1177-6>
- Rojas-Hernández S, et al. (2020) Identification of Immunogenic Antigens of *Naegleria fowleri* Adjuvanted by Cholera Toxin. *Pathogens* (Basel, Switzerland) 9(6). <https://doi.org/10.3390/pathogens9060460>
- Schorey JS, Harding CV (2016) Extracellular vesicles and infectious diseases: new complexity to an old story. *J Clin Invest* 126(4):1181–1189. <https://doi.org/10.1172/jci81132>
- Schwechheimer C, Kuehn MJ (2015) Outer-membrane vesicles from Gram-negative bacteria: biogenesis and functions. *Nat Rev Microbiol* 13(10):605–619. <https://doi.org/10.1038/nrmicro3525>
- Seong GS, Sohn HJ, Kang H, Seo GE, Kim JH, Shin HJ (2017) Production and characterization of monoclonal antibodies against cathepsin B and cathepsin B-Like proteins of *Naegleria fowleri*. *Exp Parasitol*. <https://doi.org/10.1016/j.exppara.2017.09.004>
- Serrano-Luna J, Piña-Vázquez C, Reyes-López M, Ortiz-Estrada G, de la Garza M (2013) Proteases from *Entamoeba* spp and Pathogenic Free-Living Amoebae as Virulence Factors. *Journal of tropical medicine* 2013:890603. <https://doi.org/10.1155/2013/890603>
- Shibayama M et al (2013) Disruption of MDCK cell tight junctions by the free-living amoeba *Naegleria fowleri*. *Microbiology* (reading, England) 159(Pt 2):392–401. <https://doi.org/10.1099/mic.0.063255-0>
- Siddiqui R, Ali IKM, Cope JR, Khan NA (2016) Biology and pathogenesis of *Naegleria fowleri*. *Acta Trop* 164:375–394. <https://doi.org/10.1016/j.actatropica.2016.09.009>
- Sohn HJ et al (2019) Cellular characterization of actin gene concerned with contact-dependent mechanisms in *Naegleria fowleri*. *Parasite Immunol* 41(8):e12631. <https://doi.org/10.1111/pim.12631>
- Trier NH, Hansen PR, Houen G (2012) Production and characterization of peptide antibodies. *Methods* 56(2):136–144
- Trier NH, Hansen PR, Houen G (2019) Peptides, Antibodies, Peptide Antibodies and More. *Int J Mol Sci* 20(24):6289. <https://doi.org/10.3390/ijms20246289>
- Vásquez-Moctezuma I, Meraz-Ríos MA, Villanueva-López CG, Magaña M, Martínez-Macias R, Sánchez-González DJ, García-Sierra F, Herrera-González NE (2010) ATP-binding cassette transporter ABCB5 gene is expressed with variability in malignant melanoma. *Actas*

- Dermo-Sifiliograficas 101(4):341–348. <https://doi.org/10.1016/j.ad.2009.12.006>
- Visvesvara GS, Moura H, Schuster FL (2007) Pathogenic and opportunistic free-living amoebae: *Acanthamoeba* spp, *Balamuthia mandrillaris*, *Naegleria fowleri*, and *Sappinia diploidea*. *FEMS Immunol Med Microbiol* 50(1):1–26. <https://doi.org/10.1111/j.1574-695X.2007.00232.x>
- Vyas IK, Jamerson M, Cabral GA, Marciano-Cabral F (2015) Identification of peptidases in highly pathogenic vs weakly pathogenic *Naegleria fowleri* amoebae. *J Eukaryotic Microbiol* 62(1):51–9. <https://doi.org/10.1111/jeu.12152>
- Wadhawan M, Singh N, Rathaur S (2014) Inhibition of cathepsin B by E-64 induces oxidative stress and apoptosis in filarial parasite. *PLoS ONE* 9(3):e93161. <https://doi.org/10.1371/journal.pone.0093161>
- Wilcox D, Mason RW (1992) Inhibition of cysteine proteinases in lysosomes and whole cells. *The Biochemical journal* 285(Pt 2):495–502. <https://doi.org/10.1042/bj2850495>
- Wu Z, Wang L, Li J, Wang L, Wu Z, Sun X (2018) Extracellular Vesicle-Mediated Communication Within Host-Parasite Interactions. *Front Immunol* 9:3066. <https://doi.org/10.3389/fimmu.2018.03066>
- Yadati T, Houben T, Bitorina A, Shiri-Sverdlov R (2020) The Ins and Outs of Cathepsins: Physiological Function and Role in Disease Management. *Cells* 9(7). <https://doi.org/10.3390/cells9071679>

Publisher's note Springer Nature remains neutral with regard to jurisdictional claims in published maps and institutional affiliations.

Springer Nature or its licensor holds exclusive rights to this article under a publishing agreement with the author(s) or other rightsholder(s); author self-archiving of the accepted manuscript version of this article is solely governed by the terms of such publishing agreement and applicable law.